Downregulation of TMEM220 Promotes Tumor Progression in Hepatocellular Carcinoma

Ting Li
Xi'an Jiaotong University
Lei Guan
Xi'an Jiaotong University
Guangbo Tang
Xi'an Jiaotong University
Bing He
University of Michigan
Lili Huang
Tongji University School of Medicine
Juan Wang
Xiangya Hospital Central South University
Mingyue Li
University of Pennsylvania Perelman School of Medicine
Yanxia Bai
Xi'an Jiaotong University Medical College First Affiliated Hospital
Xinyuan Li
University of Pennsylvania Perelman School of Medicine
Huqin Zhang (huqzhang@mail.xjtu.edu.cn)
Xi'an Jiaotong University https://orcid.org/0000-0001-7963-1179

Research article

Keywords: TMEM220, HCC

Posted Date: February 19th, 2021

DOI: https://doi.org/10.21203/rs.3.rs-221265/v1

Abstract

Background: In the process of long-term carcinogenesis, cells accumulate many mutations. Deregulated genes expression causes profound changes in cell proliferation, which is one of the hallmarks of HCC. Comprehensive understanding of these changes will contribute to the molecular mechanism of HCC progression.

Methods: Western blot and real-time PCR analyses were performed to examine the TMEM220 expression in HCC. Patients' transcript profiling was used to identify gene cohorts related to TMEM220. Reverse phase protein arrays (RPPA) were preformed to obtain expression data for TMEM220 relevant proteins. The effect of TMEM220 on tumor growth and metastasis were analyzed by in vitro and in vivo studies.

Results: Through clinical sample analysis, we found that TMEM220 is downregulated in tumor and lower levels of TMEM220 is associated with poor prognosis in HCC patients. Through overexpressing TMEM220 in HCC cell lines, we found that the proliferation of cancer cells was significantly slowed down and metastasis was significantly reduced. For further study of its molecular mechanism, we performed Reverse Phase Protein Array (RPPA). The results suggest that phenotypic changes caused by TMEM220 in HCC cells might be associated with FOXO and PI3K-Akt pathways. Mechanism studies showed that overexpression of TMEM220 could regulate β-catenin and FOXO3 transcriptional activity by altering their subcellular localization, affecting the expression of downstream gene p21 and SNAIL, and ultimately reducing the progression of HCC.

Conclusion: Altogether, our study proposes a working model in which upregulation of TMEM220 expression alters the genes expression involved in cell proliferation, thereby inhibiting HCC progression, which suggests that TMEM220 might serve as a clinical biomarker.

Introduction

At present, hepatocellular carcinoma (HCC) is one of the most common malignant tumors in the world, and its mortality rate is very high in Asia, Africa and Southern Europe[1]. However, due to the advanced stage at the time of diagnosis, most HCC patients have lost the opportunity of surgical treatment. Therefore, the early diagnosis of HCC patients needs to be improved.

Deregulated proliferation and aberrant metabolism are major features of cancer cells[2, 3]. Understanding of how these events in cancer cells occur synchronously is important for developing effective clinical therapies[4, 5]. So far, many signaling pathways have been found to play an important role during the progress of HCC including β-catenin and FOXO3 pathway. Nuclear accumulation of β-catenin has been found in 17–40% of HCCs[6–8], and its downstream gene *SNAIL* has been implicated in the process of epithelial mesenchymal transition (EMT) and promote metastasis[9–11]. p21, the target gene of FOXO3 pathway, is a well-known cell cycle suppressor protein[12–14]. However, the underlying molecular mechanisms by which these pathways are activated or inhibited in HCC has not been well defined yet.

Transmembrane protein 220 (TMEM220) is a family member of TMEMs that spans the entire width of the lipid bilayer and is permanently anchored. Many TMEMs from mammalian cells are well characterized in term of biological functions and structures[15–18], like G protein-coupled receptors (GPCR)[19–21], while the subcellular localization, physiological function and its role in cancer of TMEM220 remain blank. Recent studies reported LncRNAs TMEM220 is associated with HCC patients survival, and TMEM220 gene expression is downregulated in gastric cancer [22, 23]. These studies suggest us that TMEM220 might be involved in tumorigenesis and development, however, the role of TMEM220 in HCC development is still unclear. Here, the aim of this study was to explore the subcellular localization, the clinical significance of HCC, and the molecular role of TMEM220 during HCC progression.

Methods

Patients and samples

120 paired tumorous and adjacent noncancerous liver samples were collected from May 2015 to October 2019 in The First Affiliated Hospital of Xi'an Jiaotong University, Xiangya Hospital of Central South University and Shanghai Tenth People's Hospital of Tongji University. Detailed clinical pathological parameters were listed in Table S1. The average age was 55.6 years, and ages range from 39 to 75. A total of 74 males and 46 females were included. There were no patients who received chemotherapy or radiotherapy before surgery excision. Informed consent was obtained from each patient, and the study protocol, which conformed to the ethical guidelines of the 1975 Declaration of Helsinki, was approved by the Institute Research Ethics Committee at The First Affiliated Hospital, Xiangya Hospital and Shanghai Tenth People's Hospital.

Data sources

Different tissue expression of TMEM220 was obtained from National Center of Biotechnology Information (NCBI) gene database (https://www.ncbi.nlm.nih.gov). TMEM220 expression trend frequency plot among different cancer types was obtained from The HIVE Lab (https://hive.biochemistry.gwu.edu/bioxpress). TMEM220 copy number in normal liver and HCC samples (Guichard Liver: normal liver n = 86; HCC n = 99; TCGA LIHC: normal liver n = 59; HCC n = 97) were obtained from Oncomine (https://www.oncomine.org). Data of mRNA expression and overall survival (normal liver n = 50; liver cancer n = 374) were obtained from The Cancer Genome Atlas Program (TCGA) and The cBio Cancer Genomics Portal (http://cbioportal.org).

Cells and Mice

Cell lines used (SMMC7721, MHCC97H and HCCLM3) were obtained from ATCC and CAS Cell Bank (http://www.cellbank.org.cn/) and routinely culture in DMEM medium and 10% FBS and 1% penicillin-

streptomycin (100μgml^{-1} penicillin and 100μgml^{-1} streptomycin). All cultures were maintained in a humidified 5%CO_2 incubator at 37°C, and routinely passaged when 80–90% confluent. All mice (C57BL/6) were housed under pathogen-free conditions and all procedures were pre-approved by Institutional Animal Care and Use Committee of Xi'an Jiaotong University.

RNA isolation, Reverse Transcription PCR (RT-PCR) and Quantitative Real-time RT-PCR (qRT-PCR)

Total RNA was extracted using TRIzol (Invitrogen) according to the manufacturer's instructions. Reverse transcription was carried out using oligo-dT primers. 18s RNA was used as internal control. Real-time PCR was performed in an Applied Biosystems 7500 system using Power SYBR Green PCR Master Mix (Applied Biosystems).

Western Blot

The cells were lysed in RIPA buffer in presence of protease inhibitor cocktail (Roche). Whole cell lysates were prepared and subjected to 12% SDS-PAGE and transferred to NC membrane (Bio-Red). The membranes were incubated overnight at 4°C with the specific antibodies (1:1000 dilution). Membranes were washed and incubated for 1 hour at room temperature with secondary antibody conjugated with peroxidase. Membrane-bound immune complexes were detected using Super ECL detection reagent on Amersham Imager 600 (GE Healthcare).

Reverse phase protein array

RPPA was performed at the MD Anderson Cancer Center core facility using 50 μg protein per sample. All of the antibodies were validated by western blotting[24]. The statistical analyses were performed using R (version 2.7.0).

Cell cycle assay

Cells were fixed with 70 % ethanol overnight at 4°C, washed with PBS, re-suspended in 500 μl PBS with 100 μgml^{-1} RNase and incubated for 30 min at 37°C. Next, 2.5 μl PI (propidium iodide) solution (10 mgml^{-1}) was added and cell cycle was analyzed by flow cytometry.

Cell viability and Colony formation assays

Cell viability was analyzed using the Cell Counting Kit-8 (CCK-8) (Dojindo). Cells at a density of 5×10^2 per well were seeded into 96-well plates and cultured in 100μl of DMEM containing 10% FBS for 5 days. 10μl of CCK-8 solution was added to each plate, and the cells were incubated for 3 hours at 37°C. The absorbance value (OD) of each well was measured at 450 nm. Cells were plated in 6-well culture plates. After incubation for 12 days at 37°C, the cells were washed twice with PBS and stained with 0.1% crystal violet solution. The number of colonies was counted under a microscope.

Migration and invasion assays

Cell motility was assessed by cell invasion and migration assays using Transwell chambers with or without Matrigel (BD, Biosciences). Cells in medium without FBS were seeded on Transwell chambers with or without Matrigel and incubated at 37°C for 15 hours. Medium containing 2% FBS was put in the lower chamber. The invasive cells attached to the lower surface of the membrane insert were fixed, stained using Giemsa and quantified.

Wound healing assay

Cells were seeded in 12-well plates and incubated until > 80% confluence. A straight wound was created by scratching with a 200-μl pipette tip. Floating cells were removed by washing with serum-free medium twice. The cells were then cultured in serum-free medium and allowed to migrate into the wound area. Images of the migrated cells were acquired with an inverted microscope (Leica).

H&E staining

Tissues were immediately fixed in 10% formalin at room temperature for 24 h. The n the samples were embedded in paraffin, sectioned and mounted on glass microscope slides. The sections were stained with hematoxylin and eosin and examined using light microscopy.

Xenograft and Metastasis Assays

HCCLM3 or MHCC97H (1.0×10^7 cells/mouse) TMEM220 over expression and control vector cell lines were subcutaneously injected into the nude mice. Tumor was measured every other day after injection and tumor volume were calculated using the formula [$(\text{small diameter})^2 \times (\text{large diameter}) \times 0.5$]. Mouse survival was analyzed using a survival analysis. For evaluate the metastasis potential of the cells to lung and liver, briefly, HCCLM3 or MHCC97H (2.0×10^6 cells/mouse) cells were suspended in PBS with calcium and magnesium and then inoculated into the nude mice by intrasplenic or tail vein injection. The mice were monitored every day and sacrificed 4–8 weeks later, and the metastatic tumor colonies in the lung and liver were measured.

Immunofluorescence

Cells were fixed with 4% paraformaldehyde (PFA) for 20 min and permeabilize with 0.1% Triton X-100 for 5 min washed with PBS. Block sample in blocking buffer (5% FBS + 1% HISS) for 60 min, and then incubated overnight at 4°C in primary antibodies. Fluorescent Alexa-Fluor-488 or -555-conjugated secondary antibodies (life technologies, Carlsbad, CA, USA) were used for detection. NIS-Elements (Nikon) were applied to reconstructs and renders 3D images from multiple Z-axis planes.

Promoter Luciferase Assay

Cells were transfected with reporter constructs containing the promoter together with expression vector or empty vector using Lipofectamine 3000 (Thermo Fisher Scientific). After 48 hours, the luciferase activities of whole cell lysates were measured using the dual-luciferase reporter assay system (Promega).

ChIP

ChIP assay was carried out using Chromatin Immunoprecipitation Kit (Sigma-Aldrich) according to the manufacturer's protocol. Briefly, Cells were fixed in 1% formaldehyde at room temperature for 10 min and lysed in the lysis buffer. Chromatin solutions were prepared with enzymatic shearing, and immunoprecipitated overnight at 4°C using 2 μg of specific antibodies or control IgG. Input and immunoprecipitated chromatins were incubated for 15 min at 95°C to reverse cross-link. After 1hour proteinase K digestion at 37°C, Proteinase K Stop Solution was added to abolish proteinase K activity. ChIP DNA was then analyzed by qPCR.

Statistics Analysis

The statistical analyses used included two-tailed unpaired Student's t-test, chi-squared test, two-way ANOVA and Mann-Whitney U-test. Data analysis was performed using the Prism 8 (GraphPad Software) and SPSS software version 26. Survival of distinct subgroups of HCCs were compared by Kaplan-Meier and log-rank analyses. Results were presented as mean ± S.D. $P < 0.05$ was considered statistically significant.

Results

TMEM220 is downregulated in human HCC and associated with poor clinical outcomes

We noticed the presence of high expression levels of TMEM220 in healthy human liver as compared to the other tissues or organs in the body (Fig. S1a), whereas TMEM220 expression was significantly decreased in tumor when compared with normal liver tissue (Fig. 1a, b). Moreover, TMEM220 gene copy number decreased and methylation of TMEM220 gene increased in HCC tissues (Fig. 1c, d and Fig. S1b). On this basis, we analyzed the expression of TMEM220 in 120 pairs of collected HCC clinical samples. Consistent with the findings above, the expression level of TMEM220 in tumor was much lower than adjacent normal livers (ANLs) (Fig. 1e), and 91.7% (110/120) of them showed under expression (Fig. 1f, g). Most importantly, by grouping the samples with TMEM220 expression level, we found that the overall survival curve of the high expression group was significantly better than that of the low expression group through 5-year follow-up (Fig. 1h and Fig. S1c). In addition, TMEM220 mRNA levels weremuch lower in SMMC7721, MHCC97H and HCCLM3 HCC cell lines compared with normal hepatic cell line (Fig. S1d), therefore we choose these 3 cell lines for subsequent research. These data suggest that the expression of TMEM220 is significantly decreased in HCC tissues, and its low expression is closely related with poor prognosis in HCC patients.

Overexpression of TMEM220 blocks HCC cell growth and decreases metastasis

Since the subcellular localization of TMEM220 is yet to be reported, using immunofluorescence, we clearly identified that TMEM220 mainly localized on the plasma membrane in HCC cells (Fig. 2a and Fig. S2).

To study the effect of TMEM220 on HCC cells, we generated HCC cell lines that overexpress TMEM220. First, cell cycle analysis by flow cytometry showed that the percentage of TMEM220 over-expressed cells at G1 stage was significantly higher than the control cells (Fig. 2b). Subsequent cell proliferation assay and colony formation assay indicated that the growth of TMEM220 overexpressed cells was slowed down markedly (Fig. 2c, d). Moreover, tumor xenograft study in nude mice showed that the tumor growth of overexpression cell was blocked (Fig. 2e), and accordingly, these mice survived longer than those of the control group (Fig. 2f). Taken together, data here suggested that overexpression of TMEM220 inhibited the growth of HCC cells both *in vitro* and *in vivo*.

In addition to growth, metastasis is another important indicator of HCC malignancy. The migration assay, invasion assay and wound healing assay results showed that the migratory and invasive capacity of TMEM220 overexpression HCC cells were decreased *in vitro* (Fig. 3a, b). At the same time, *in vivo* metastasis assay showed that the liver metastasis (Fig. 4c) and lung metastasis (Fig. 4d) of TMEM220 overexpressed cells were significantly reduced. These data suggested that overexpression of TMEM220 suppressed metastasis in HCC cells.

Signaling downstream of TMEM220 in HCC

To further explore the role of TMEM220 in HCC, we performed Reverse Phase Protein Array (RPPA) in TMEM220 overexpression SMMC7721 cell lines and control cell lines (Table S2). Based on the RPPA results, we found 131 altered proteins ($P < 0.05$; more than 1.5-fold change), 58 of which were upregulated or phosphorylation levels were increased, while 73 were downregulated or phosphorylation levels were decreased (Fig. S3a). Some of the altered proteins (Fig. 4a) were verified by Western blot in MHCC97H and HCCLM3 (Fig. 4b). Furthermore, the protein-protein interaction (PPI) network is established to investigate the signal network affected by TMEM220 (Fig. 4c and Fig. S3b, c). The proteins that were upregulated or had increased phosphorylation levels in TMEM220 over expression cells were significantly enriched in FOXO signaling pathway (Fig. 4d upper panel), whereas the proteins that were downregulated or had decreased phosphorylation levels were highly enriched in PI3K-Akt signaling pathway (Fig. 4d lower panel). CDKN1A (p21), PTEN and FOXO3 (FOXO3-pS318/321 inactive form decreased) were involved in the activated PPI subset (Fig. S3b), while PCNA, AKT, MAPK and β-catenin (β-catenin pT41/S45 inactive form increased) were present in the inactivated subset (Fig. S3c). Data reported here indicated that TMEM220 might be involved in HCC progression through PI3K-Akt and FOXO3 pathways.

TMEM220 affect downstream gene expression by altering β-catenin and FOXO3 subcellular localization

The RPPA result of over-expressed TMEM220 suggested that TMEM220 might function via regulating two hub transcription factors, β-catenin and FOXO3. RPPA results also implicated that TMEM220 overexpression also can inhibit AKT and GSK3β phosphorylation. So we proposed that TMEM220 could regulate the activity of these two transcription factors.

We first examined the effect of TMEM220 on subcellular localization of β-catenin. When transfected with TMEM220, β-catenin was translocated from the nucleus to the cytoplasm; and if the cells were treated with BIO (GSK3β inhibitor), the rate of nuclear-cytoplasmic shuttling of β-catenin could be blocked efficiently (Fig. 5a-c). Meanwhile, TOPFALSH/FOPFLASH reporter assay showed that the transcription activity of β-catenin induced by Wnt3a or β-catenin was gradually suppressed by TMEM220 over expression (Fig. S4a, b). β-catenin S33Y, which is insensitive to GSK-3β, abrogated the inhibition due to TMEM220 (Fig. S4c). Moreover, TMEM220 overexpression could inhibit Snail expression, which is a β-catenin downstream gene related to epithelial-to-mesenchymal transition (EMT) in HCC (Fig. S4d). Collectively, these results suggested that TMEM220 might negatively regulates β-catenin mediated EMT acts through AKT-GSK3β cascade.

On the other hand, we found that overexpression of TMEM220 also changed the sub cellular localization of FOXO3. However, FOXO3 is transferred from the cytoplasm to the nucleus (Fig. 5e, f). Consistently, the phosphorylation level of FOXO3, its inactivated form, was decreased with TMEM220 overexpression (Fig. 4b). Correspondingly, TMEM220 overexpression increased FOXO3 binding on p21 (FOXO3 target gene) promoter and activated its expression (Fig. 5g, h). Consistent with critical cyclin-dependent kinase (Cdk) inhibitory roles for p21, p21 arrests cell cycle by blocking the G1 phase (Fig. 2b). Collectively, our data implicated that TMEM220 could promote FOXO3 nuclear accumulation and increase p21 to inhibit HCC cell growth.

Discussion

In this study, first, we found that TMEM220 showed significant low expression in HCC and was associated with poor prognosis. Subsequent studies showed that TMEM220 overexpression could block the growth and metastasis *in vitro* and *in vivo*. To further study the molecular mechanisms underlying the effects of TMEM220 in HCC, we used RPPA to analyze its associated signaling networks in HCC cell lines. We found that TMEM220 may influence downstream genes expression by regulating FOXO3 and β-catenin activities. Consistently, emerging evidences indicate that FOXO3 acts as a tumor suppressor in cancer by promoting p21 transcription, and β-catenin promotes metastasis in HCC[25, 26]. Collectively, results reported in this study promoted us to propose a new working model of the role of TMEM220 in HCC progression (Fig. S4d). Over expression of TMEM220 leads to β-catenin inhibition and FOXO3 activation, and inhibits metastasis and cell proliferation in HCC cell lines.

TMEM220 similar to other TMEM family members, such as TMEM97 and TMEM98, could increase PTEN and suppress AKT axes[15, 27]. However, the upstream mechanisms of these TMEMs/AKT axes remain elusive. In this study, RPPA results suggest that TMEM220 over expression increases PTEN and inhibits AKT phosphorylation. As a consequence, GSK3β cannot be suppressed by AKT, and then inhibit β-catenin function. Meanwhile, AKT-mediated phosphorylation of FOXO3 has been blocked, thereby promoting the expression of its gene targets such as P21. Moreover, RPPA data have shown that the phosphorylation of c-MET (Y1234/1235) could be inhibited by TMEM220 overexpression in HCC (Fig. 4a, b). C-MET (mesenchymal-epithelial transition factor/scatter factor receptor), which ligand is HGF/SF (ligand

hepatocyte growth factor/scatter factor), can trigger various of downstream signaling pathways, such as PI3K/AKT, JAK/STAT, Ras/MAPK, and GSK3β/β-catenin[28–30]. The question arises as to how TMEM220 inhibits the activation of c-MET. Given that an increased level of intracellular calcium could negatively regulate c-MET[31], one candidate mechanism is that TMEM220, like some other TMEMs such as TMEM176A/B which also have four transmembrane helical domain like TMEM220, might act as a cation channel to control the cytosolic calcium level, thereby suppressing the c-MET activation[32].

Conclusion

Altogether, our study has shown that TMEM220 is decreased in tumor and associated with poor prognosis in HCC. Based on our finding, we proposed a working model in which upregulation of TMEM220 expression alters the genes expression involved in cell proliferation, thereby inhibiting HCC progression. Taken together, data reported here suggests that TMEM220 might serve as a prognostic marker for HCC treatment improvement.

Abbreviations

TMEM, transmembrane protein; HCC, hepatocellular carcinoma; ChIP, chromatin immunoprecipitation; RPPA, reverse phase protein array; TCGA-LIHC, the cancer genome atlas liver hepatocellular carcinoma; PPI, psychophysiological interactions; EMT, epithelial to mesenchymal transition; GO, Gene Ontology.

Declarations

Ethics approval and consent to participate

Each patient consented to the approved protocol which confirmed by the Institute Research Ethics Committee at The First Affiliated Hospital, Xiangya Hospital and Shanghai Tenth People's Hospital.

Consent for publication

All authors have agreed to publish this manuscript.

Availability of data and material

The datasets generated and/or analyzed during the current study are involved in this published article (and its supplementary information files) or available on published databases (TCGA).

Competing interests

No potential conflicts of interest were disclosed.

Authors' contributions:

Conception and design: X.Y.L. and H.Q.Z.; Acquisition of data (provided animals, acquired and managed patients, provided facilities, etc.): T.L., L.G., G.B.T., B.H., J.W., L.L.H., M.Y.L., Y.X.B.; Analysis and interpretation of data (e.g., statistical analysis, biostatistics, computational analysis):T.L., G.L., J.W., B.H., J.P.W.; Technical, or material support (reporting or organizing data, constructing databases): S.S.D..

Acknowledgements:

We thank Professor Tie-lin Yang, Yan Guo at Xi'an Jiaotong University for helpful data analysis. This work was supported by the National Natural Science Foundation of China (Grant No. 61372151 and Grant No. 31570917).

Authors' information

Ting Li and Lei Guan contributed equally to this work.

Correspondence to Huqin Zhang.

References

1. Jemal, A., et al., *Global cancer statistics.* CA Cancer J Clin, 2011. **61**(2): p. 69-90.
2. Yang, J., et al., *The enhancement of glycolysis regulates pancreatic cancer metastasis.* Cell Mol Life Sci, 2020. **77**(2): p. 305-321.
3. Green, D.R. and G.I. Evan, *A matter of life and death.* Cancer Cell, 2002. **1**(1): p. 19-30.
4. Morandi, A. and S. Indraccolo, *Linking metabolic reprogramming to therapy resistance in cancer.* Biochim Biophys Acta Rev Cancer, 2017. **1868**(1): p. 1-6.
5. Deshmukh, A., et al., *Cancer stem cell metabolism: a potential target for cancer therapy.* Mol Cancer, 2016. **15**(1): p. 69.
6. Breuhahn, K. and P. Schirmacher, *Signaling networks in human hepatocarcinogenesis--novel aspects and therapeutic options.* Prog Mol Biol Transl Sci, 2010. **97**: p. 251-77.
7. Galuppo, R., et al., *Synergistic inhibition of HCC and liver cancer stem cell proliferation by targeting RAS/RAF/MAPK and WNT/beta-catenin pathways.* Anticancer Res, 2014. **34**(4): p. 1709-13.
8. Khalaf, A.M., et al., *Role of Wnt/beta-catenin signaling in hepatocellular carcinoma, pathogenesis, and clinical significance.* J Hepatocell Carcinoma, 2018. **5**: p. 61-73.
9. Cao, F. and L.X. Yin, *PAK1 promotes proliferation, migration and invasion of hepatocellular carcinoma by facilitating EMT via directly up-regulating Snail.* Genomics, 2020. **112**(1): p. 694-702.

10. Wang, Y., et al., *The Role of Snail in EMT and Tumorigenesis.* Curr Cancer Drug Targets, 2013. **13**(9): p. 963-972.
11. Zhang, Y., et al., *SNHG7 accelerates cell migration and invasion through regulating miR-34a-Snail-EMT axis in gastric cancer.* Cell Cycle, 2020. **19**(1): p. 142-152.
12. Sato, A., et al., *Glioma-initiating cell elimination by metformin activation of FOXO3 via AMPK.* Stem Cells Transl Med, 2012. **1**(11): p. 811-24.
13. Du, W.W., et al., *Foxo3 circular RNA retards cell cycle progression via forming ternary complexes with p21 and CDK2.* Nucleic Acids Res, 2016. **44**(6): p. 2846-58.
14. Zhang, X., et al., *Akt, FoxO and regulation of apoptosis.* Biochim Biophys Acta, 2011. **1813**(11): p. 1978-86.
15. Schmit, K. and C. Michiels, *TMEM Proteins in Cancer: A Review.* Front Pharmacol, 2018. **9**: p. 1345.
16. Marx, S., et al., *Transmembrane (TMEM) protein family members: Poorly characterized even if essential for the metastatic process.* Semin Cancer Biol, 2020. **60**: p. 96-106.
17. Zhang, Z., et al., *The conserved transmembrane protein TMEM-39 coordinates with COPII to promote collagen secretion and regulate ER stress response.* PLoS Genet, 2021. **17**(2): p. e1009317.
18. Xu, J., et al., *Inhibition of Proliferation by Knockdown of Transmembrane (TMEM) 168 in Glioblastoma Cells via Suppression of Wnt/beta-Catenin Pathway.* Oncol Res, 2019. **27**(7): p. 819-826.
19. Shimada, I., et al., *GPCR drug discovery: integrating solution NMR data with crystal and cryo-EM structures.* Nat Rev Drug Discov, 2019. **18**(1): p. 59-82.
20. Wootten, D., et al., *Mechanisms of signalling and biased agonism in G protein-coupled receptors.* Nat Rev Mol Cell Biol, 2018. **19**(10): p. 638-653.
21. Pluimer, B.R., M. Colt, and Z. Zhao, *G Protein-Coupled Receptors in the Mammalian Blood-Brain Barrier.* Front Cell Neurosci, 2020. **14**: p. 139.
22. Choi, B., et al., *MAL and TMEM220 are novel DNA methylation markers in human gastric cancer.* Biomarkers, 2017. **22**(1): p. 35-44.
23. Wang, Z., et al., *Identification of four prognostic LncRNAs for survival prediction of patients with hepatocellular carcinoma.* PeerJ, 2017. **5**: p. e3575.
24. Tibes, R., et al., *Reverse phase protein array: validation of a novel proteomic technology and utility for analysis of primary leukemia specimens and hematopoietic stem cells.* Mol Cancer Ther, 2006. **5**(10): p. 2512-21.
25. Liu, L., et al., *Activation of beta-catenin by hypoxia in hepatocellular carcinoma contributes to enhanced metastatic potential and poor prognosis.* Clin Cancer Res, 2010. **16**(10): p. 2740-50.
26. Yuan, K., et al., *TXNDC12 promotes EMT and metastasis of hepatocellular carcinoma cells via activation of beta-catenin.* Cell Death Differ, 2020. **27**(4): p. 1355-1368.
27. Oyer, H.M., C.M. Sanders, and F.J. Kim, *Small-Molecule Modulators of Sigma1 and Sigma2/TMEM97 in the Context of Cancer: Foundational Concepts and Emerging Themes.* Front Pharmacol, 2019. **10**:

p. 1141.

28. Li, N., et al., *Helicobacter pylori CagA Protein Negatively Regulates Autophagy and Promotes Inflammatory Response via c-Met-PI3K/Akt-mTOR Signaling Pathway.* Front Cell Infect Microbiol, 2017. **7**: p. 417.
29. Stevenson, N.J., et al., *Hepatitis C virus targets the interferon-alpha JAK/STAT pathway by promoting proteasomal degradation in immune cells and hepatocytes.* FEBS Lett, 2013. **587**(10): p. 1571-8.
30. Rotow, J.K., et al., *Co-occurring Alterations in the RAS-MAPK Pathway Limit Response to MET Inhibitor Treatment in MET Exon 14 Skipping Mutation-Positive Lung Cancer.* Clin Cancer Res, 2020. **26**(2): p. 439-449.
31. Gomes, D.A., et al., *c-Met must translocate to the nucleus to initiate calcium signals.* J Biol Chem, 2008. **283**(7): p. 4344-51.
32. Picotto, G., et al., *TMEM176A and TMEM176B Are Candidate Regulators of Inhibition of Dendritic Cell Maturation and Function after Chronic Spinal Cord Injury.* J Neurotrauma, 2020. **37**(3): p. 528-533.

Figures

Fig.1

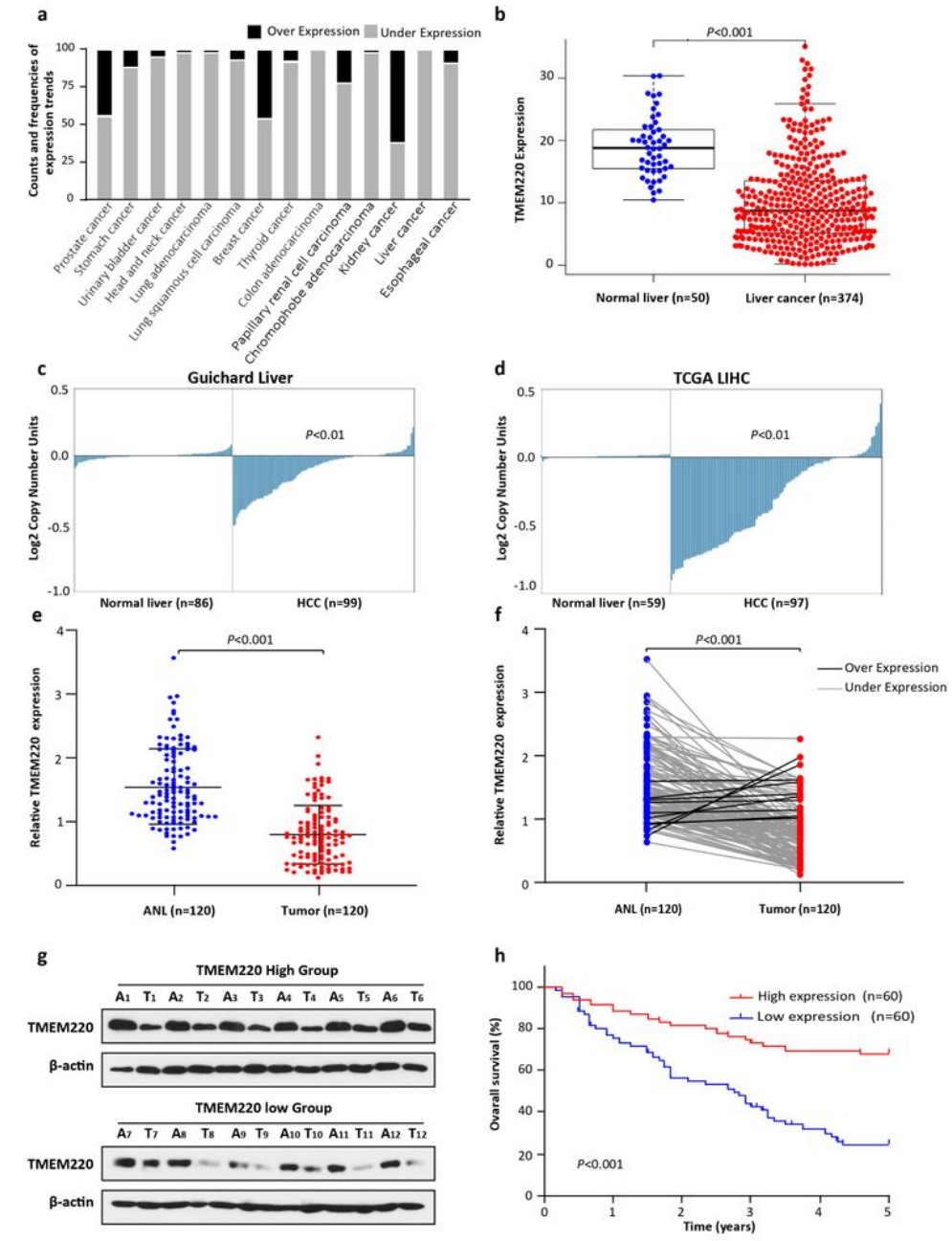

Figure 1

TMEM220 is downregulated in human HCC and associated with poor clinical outcomes. a Expression trend frequencies for TMEM220 in different cancer types from BioXpress (https://hive.biochemistry.gwu.edu/tools/bioxpress). b The Cancer Genome Atlas (TCGA) Liver Hepatocellular Carcinoma (LIHC) data indicating TMEM220 expression in Normal liver (n=50) vs. Liver cancer (n=374). c and d TMEM220 gene copy numbers in normal liver and HCC in the Guichard Liver

microarray and TCGA LIHC (Oncomine database). e TMEM220 mRNA expression was determined for 120 pairs of matched ANL and tumor tissues in collected HCC patients by PCR. f Comparation of TMEM220 expression trend in paired ANL and tumor tissues in e. g Representative TMEM220 expression levels in paired A (ANL) and T (Tumor) tissues in collected HCC patients by western blot. h Kaplan-Meier survival curves in relation to the expression levels of TMEM220 expression in collected HCC patients.

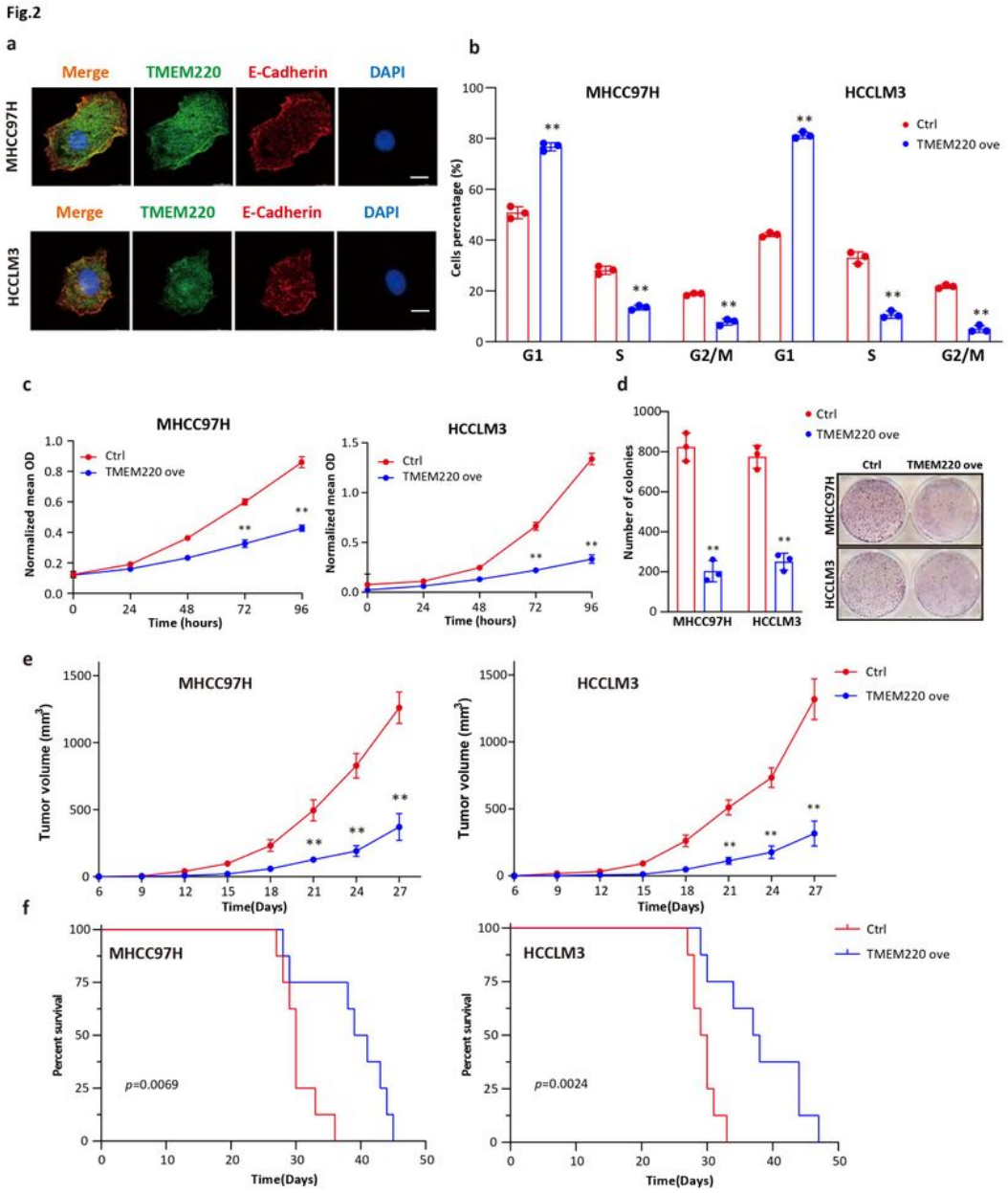

Figure 2

TMEM220 overexpression suppresses HCC proliferation in vivo and in vitro. a Subcellular localization of TMEM220 in HCC cells (MHCC97H upper panel and HCCLM3 lower panel) determined by immunofluorescence. TMEM220 and plasma membrane marker (E-Cadherin) were co-stained with 4',6-diamidino-2-phenylindole (blue) and anti-TMEM220 (green) or anti-E-Cadherin (red) immunoglobulin G secondary antibody conjugates. Scale bar=10μm. b Cell cycle analysis of TMEM220 overexpression propidium iodide-stained cells compare with control cells by flow cytometry. c Proliferation of TMEM220 overexpression cells compare with control cells by Cell Counting Kit-8 (CCK-8) assay. d Colony formation of TMEM220 overexpression cells compare with control cells. e Tumor growth in nude mice that were injected subcutaneously with indicated cell lines (n=8). Statistical significance was determined by two-way ANOVA. f Survival curve of mice in e using Log-rank (mantel-cox) test.

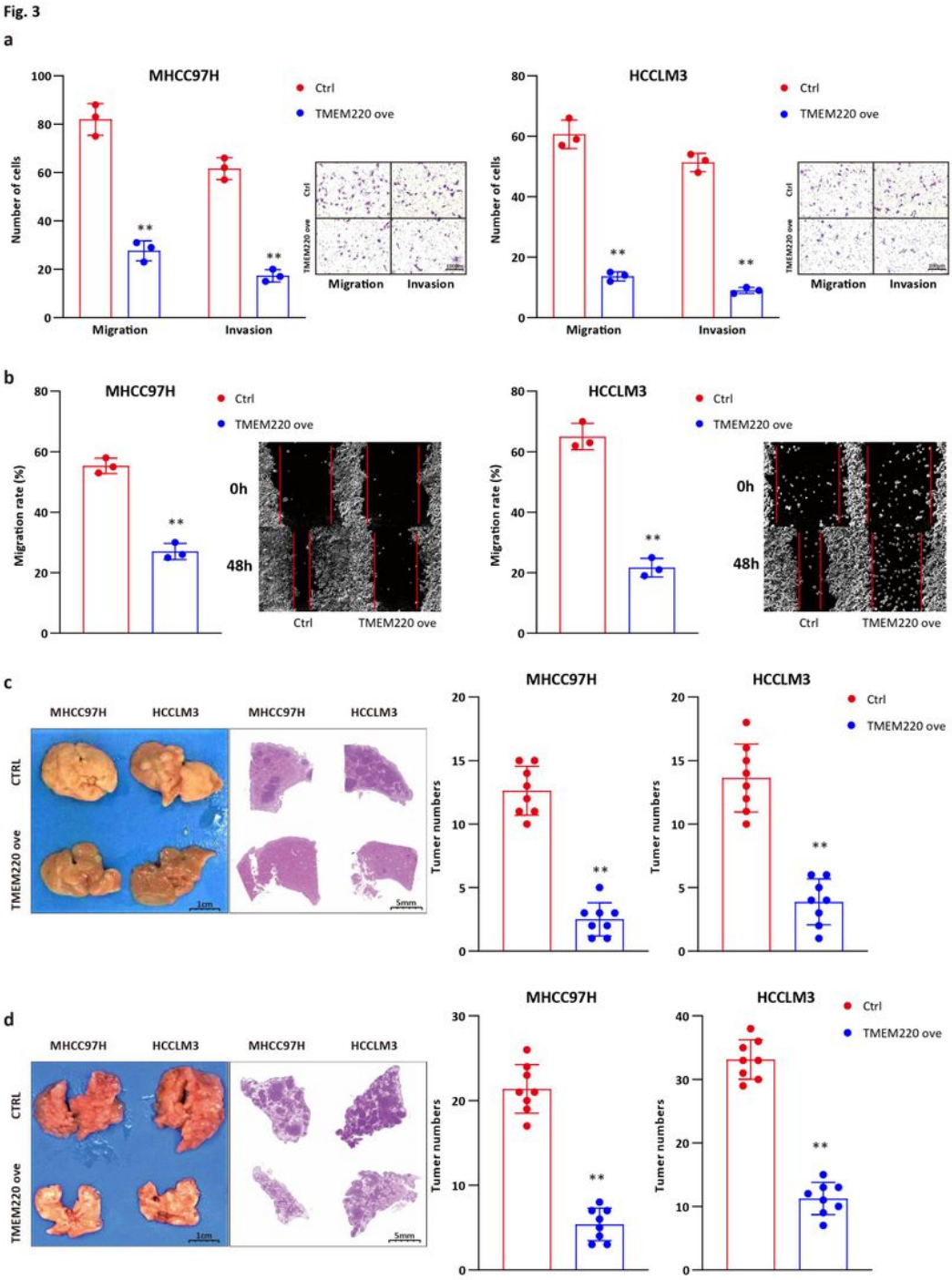

Figure 3

TMEM220 overexpression suppresses HCC metastasis in vivo and in vitro. a and b Migration and invasion assays (a) and Wound healing assay (b) of TMEM220 overexpression cells compare with control cells using Transwell membrane without or with Matrigel respectively. Scale bar=100μm. c and d Representative image & H&E staining and tumor nodules numbers of liver (c) or lung (d) metastasis in

nude mice metastasis model by intrasplenic or tail vein injection for indicated cell lines (n=8). *P< 0.05, ** P < 0.01 (two-tailed t test).

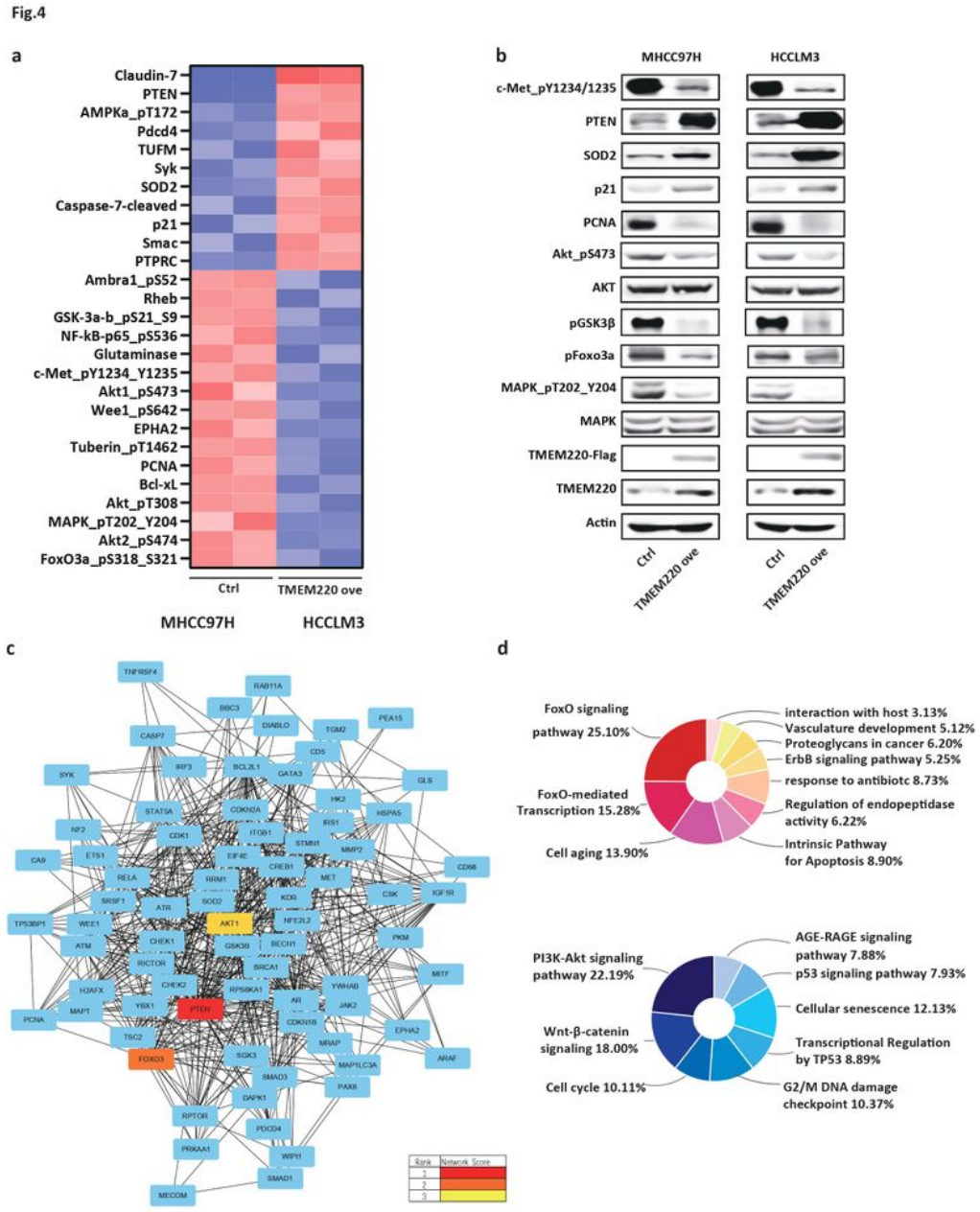

Figure 4

Protein profiling affected by TMEM220 overexpression in HCC. a Heat map of the indicated proteins in control (ctrl) compared with TMEM220 stable over expression (TMEM220 ove) SMMC7721 cells by Reverse phase protein array (RPPA). b Indicated proteins levels were detected in MHCC97H and HCCLM3

cells by Western blot. c The protein-protein interaction (PPI) network and top3 hub genes were ranked by mixed character calculation (MCC) method (cytoHubber). A cutoff fold change of ≥1.5 or ≤−1.5 and P value of ≤0.01 were applied, and only proteins that met these criteria were selected. d Pathway enrichment analysis of the proteins changed in TMEM220 over expression SMMC7721 cells (upregulated protein, upper panel; downregulated protein, lower panel).

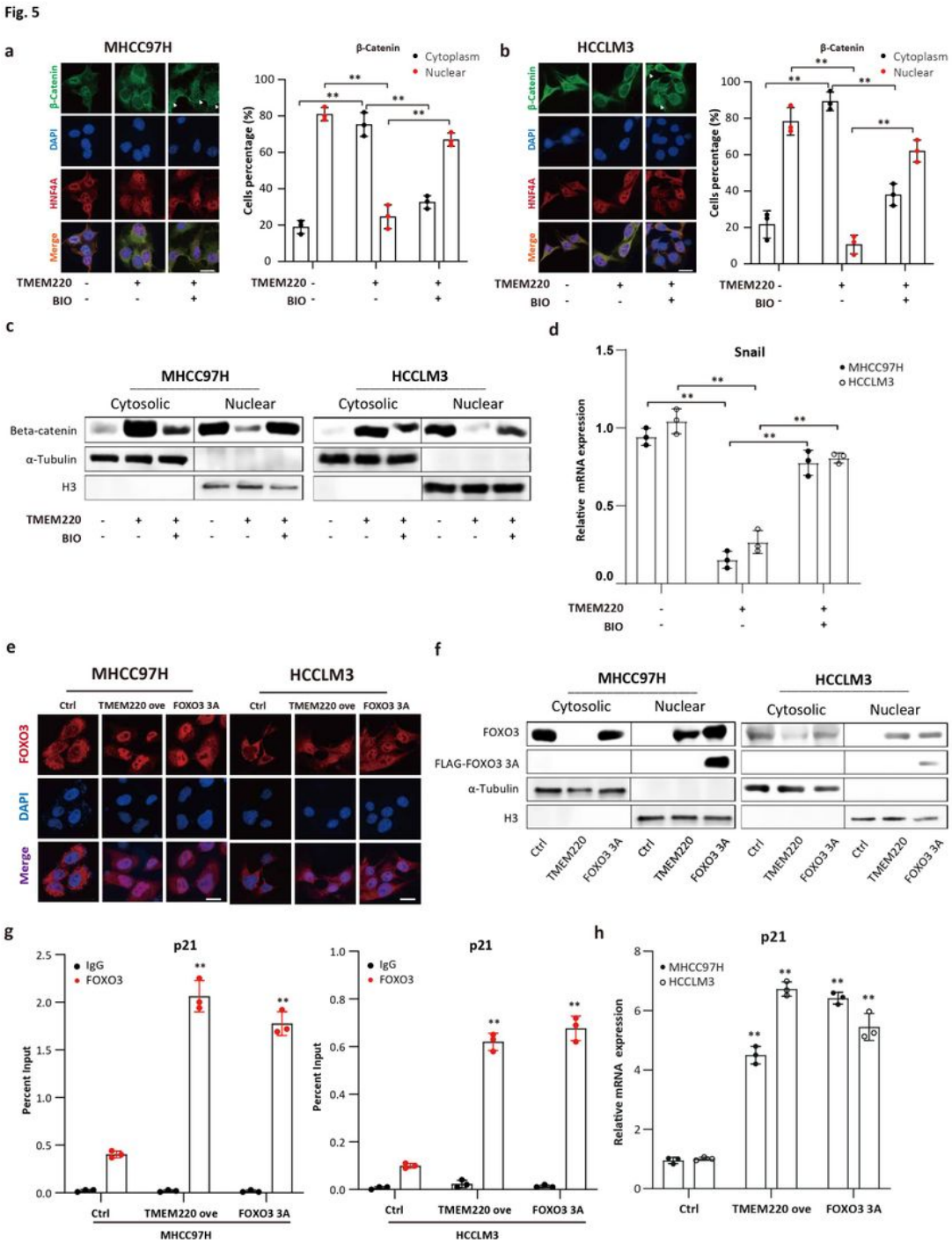

Figure 5

TMEM22 overexpression affects β-catenin and FOXO3 subcellular localization and downstream gene expression a and b β-catenin subcellular localization detected by immunofluorescence in control and TMEM220 overexpression MHCC97H cells (a) and HCCLM3 (b). c β-catenin subcellular localization detected by western blot. d Snail mRNA expression levels of HCC cell lines under indicated treatment determined by PCR. e FOXO3 subcellular localization detected by immunofluorescence in control and TMEM220 overexpression MHCC97H cells (left) and HCCLM3 (right). f FOXO3 subcellular localization detected by western blot. g FOXO3 binding to the p21 promoter regions in HCC cells with indicated treatment determined by ChIP. h p21 mRNA expression levels of HCC cell lines under indicated treatment determined by PCR. For a, b and e, the percentage of cells with nuclear-localized β-catenin/FOXO3 was calculated from 50 cells in five different fields for each experiment (right). Scale bar=10μm. For all panels, experiments were repeated 3 times. Data are presented as the mean ± s.e.m. *P< 0.05, ** P < 0.01

Supplementary Files

This is a list of supplementary files associated with this preprint. Click to download.

- Supplementaryinformationprimerandantibodies.pdf
- Supplementarytable1.pdf
- Supplementarytable2.pdf
- Supplementarytable3.pdf
- supplementalfig02072021.pdf